Foundation Teacher-Scholar Grant (1970–1975). We also thank Mr. John Sexauer for the synthesis of the complexes $K_3W_2Cl_9$, $(Et_4N)_3Rh_2Cl_9$, and $Rb_3Mo_2Cl_8H$ and Professor R. A. D. Wentworth, who kindly provided us with samples of $(Bu_4N)_3M_2Cl_9$, where M = Cr, Mo, or W.

Registry No. **1**, 38845-35-1; **2**, 60260-34-6; **3**, 60260-33-5; **4**, 16843-37-1; **5**, 60260-32-4; **6**, 28681-19-8; **7**, 60260-28-8; **8**, 14023-10-0; **9**, 12016-49-8; **10**, 10534-89-1; **11**, 13408-73-6; **12**, 13859-51-3; **13**, 13820-95-6; **14**, 13782-02-0; **15**, 21288-85-7; **16**, 14040-33-6; **17**, 60260-26-6; **18**, 60260-43-7; **19**, 14077-30-6; **20**, 14406-85-0; **21**, 20647-35-2; **24**, 60260-42-6; **25**, 49732-12-9; **26**, 19121-74-5; **27**, 13774-14-6.

References and Notes

(1) Part 11: J. R. Ebner, D. L. McFadden, and R. A. Walton, *J. Solid-State Chem.*, **17**, 447 (1976).
(2) Part 10: J. R. Ebner and R. A. Walton, *Inorg. Chem.*, **14**, 2289 (1975).
(3) B. Folkesson, *Acta Chem. Scand.*, **27**, 287, 1441 (1973).
(4) E. I. Solomon, P. J. Clendening, H. B. Gray, and F. J. Grunthaner, *J. Am. Chem. Soc.*, **97**, 3878 (1975).
(5) H. D. Glicksman and R. A. Walton, *Inorg. Chim. Acta*, **19**, 91 (1976).
(6) A. D. Hamer and R. A. Walton, *Inorg. Chem.*, **13**, 1446 (1974).
(7) D. G. Tisley and R. A. Walton, *Inorg. Chem.*, **12**, 373 (1973).
(8) D. G. Tisley and R. A. Walton, *J. Inorg. Nucl. Chem.*, **35**, 1905 (1973).
(9) A. D. Hamer, D. G. Tisley, and R. A. Walton, *J. Inorg. Nucl. Chem.*, **36**, 1771 (1974).
(10) D. G. Tisley and R. A. Walton, *J. Chem. Soc., Dalton Trans.*, 1039 (1973).
(11) M. J. Bennett, J. V. Brencic, and F. A. Cotton, *Inorg. Chem.*, **8**, 1060 (1969).
(12) R. J. Ziegler and W. M. Risen, Jr., *Inorg. Chem.*, **11**, 2796 (1972).
(13) R. A. Work, III, and M. L. Good, *Inorg. Chem.*, **9**. 956 (1970).
(14) At the time we started this work, the molybdenum complex $Rb_3Mo_2Cl_8H$ was formulated[11] as $Rb_3Mo_2Cl_8$. It is only recently[15] that it has been identified as a hydride derivative, with the H^- ligand occupying one of the bridging positions between the molybdenum atoms.
(15) F. A. Cotton and B. J. Kalbacher, *Inorg. Chem.*, **15**, 522 (1976).
(16) H. Yamatera and K. Nakatsu, *Bull. Chem. Soc. Jpn.*, **27**, 244 (1954).
(17) J. Bjerrum and J. P. McReynolds, *Inorg. Synth.*, **2**, 217 (1946).
(18) J. B. Work, *Inorg. Synth*, **2**, 221 (1946).
(19) W. L. Jolly, "The Synthesis and Characterization of Inorganic Compounds", Prentice-Hall, Englewood Cliffs, N.J., 1970, p 463.
(20) J. C. Bailar, Jr., *Inorg. Synth.*, **2**, 222 (1946).
(21) S. M. Jorgensen, *J. Prakt. Chem.*, **41**, 440 (1890).
(22) J. A. Osborn, K. Thomas, and G. Wilkinson, *Inorg. Synth.*, **13**, 213 (1972).
(23) S. N. Anderson and F. Basolo, *Inorg. Synth.*, **7**, 216 (1963).
(24) R. D. Gillard and G. Wilkinson, *Inorg. Synth.*, **10**, 64 (1967).
(25) F. H. Burstall and R. S. Nyholm, *J. Chem. Soc.*, 3570 (1952).
(26) H. M. State, *Inorg. Synth.*, **6**, 198 (1960).
(27) H. M. Powell and A. F. Wells, *J. Chem. Soc.*, 359 (1935).
(28) J. T. Veal and D. J. Hodgson, *Inorg. Chem.*, **11**, 597 (1972).
(29) G. C. Allen and N. S. Hush, *Inorg. Chem.*, **6**, 4 (1967).
(30) D. W. Meek and J. A. Ibers, *Inorg. Chem.*, **9**, 465 (1970).
(31) F. A. Cotton and D. A. Ucko, *Inorg. Chim. Acta*, **6**, 161 (1972), and references therein.
(32) I. E. Grey and P. W. Smith, *Aust, J. Chem.*, **24**, 73 (1971), and references therein.
(33) R. Saillant, R. B. Jackson, W. E. Streib, K. Folting, and R. A. D. Wentworth, *Inorg. Chem.*, **10**, 1453 (1971).
(34) For a full listing of all the relative peak intensities see J. R. Ebner, Ph.D. Thesis, Purdue University, 1975, p 111.
(35) F. A. Cotton and J. T. Mague, *Inorg. Chem.*, **3**, 1094 (1964).
(36) P. F. Stokely, Ph.D. Thesis, Massachusetts Institute of Technology, 1969.
(37) W. H. Watson, Jr., and J. Waser, *Acta Crystallogr.*, **11**, 689 (1958).
(38) T. Birchall, J. A. Connor, and I. H. Hillier, *J. Chem. Soc., Dalton Trans.*, 2003 (1975).
(39) S. K. Porter and R. A. Jacobson, *J. Chem. Soc. A*, 1359 (1970).
(40) A. D. Hamer, D. G. Tisley, and R. A. Walton, *J. Chem. Soc., Dalton Trans.*, 116 (1973).
(41) A. S. Antsyshkina and M. A. Porai-Koshits, *Dokl. Akad. Nauk SSSR*, **143**, 105 (1962).
(42) G. G. Messmer and E. L. Amma, *Acta Crystallogr., Sect. B*, **24**, 417 (1968).
(43) I. A. Baidina, N. V. Podberezskaya, and L. P. Solov'eva, *J. Struct. Chem. (USSR)*, **15**, 834 (1974).
(44) K. Burger, E. Fluck, H. Binder, and Cs. Várhelyi, *J. Inorg. Nucl. Chem.*, **37**, 55 (1975).
(45) V. I. Nefedov, E. F. Shubochkina, I. S. Kolomnikov, I. R. Baranovskii, V. P. Kukolev, M. A. Golubinchaya, L. K. Shubochkin, M. A. Porai-Koshits and M. E. Vol'pin, *Russ. J. Inorg. Chem. (Engl. Transl.)*, **18**, 444 (1973).
(46) As with much of the XPS data in the literature, those reported in ref 45 list the relevant binding energies but give no information on peak shapes or peak widths.
(47) S. O. Grim, L. J. Matienzo, and W. E. Swartz, Jr., *Inorg. Chem.*, **13**, 447 (1974).
(48) V. I. Nefedov, I. V. Prokof'eva, A. E. Bukanova, L. K. Shubochkin, Ya. V. Salyn', and V. L. Pershin, *Russ. J. Inorg. Chem. (Engl. Transl.)*, **19**, 859 (1974).
(49) B. Zaslow and G. L. Ferguson, *Acta Crystallogr., Sect B*, **27**, 849 (1971).
(50) B. N. Figgis, M. Gerloch, and R. Mason, *Proc. R. Soc. London, Ser. A*, **279**, 210 (1964).
(51) D. A. Shirley, *Chem. Phys. Lett.*, **16**, 220 (1972).
(52) K. S. Kim and N. Winograd, *Chem. Phys. Lett.*, **30**, 91 (1975), and references therein.
(53) R. A. Walton, "Proceedings of the Second International Conference on the Chemistry and Uses of Molybdenum", P. C. H. Mitchell, Ed., Oxford University, in press.
(54) A. D. Hamer, Ph.D. Thesis, Purdue University, 1974.

Contribution from the Department of Chemistry, University of Maine, Orono, Maine 04473

Optical Spectra of the Tetrabromopalladate(II) Ion Doped in Cesium Hexabromozirconate(IV) at 2 K

THOMAS G. HARRISON, HOWARD H. PATTERSON,* and MARTHA T. HSU

Received March 22, 1976 AIC60217B

The optical spectra of the tetrabromopalladate(II) ion doped as a substitutional impurity in cesium hexabromozirconate(IV) has been measured at 2 K. An electronic band has been observed between 19 185 and 21 836 cm^{-1} with sharp vibrational detail and is assigned as the d–d transition, $\Gamma_1(^1A_{1g}) \rightarrow \Gamma_2(^1A_{2g})$. The mixed crystal vibrational data for this band has been compared with recent single crystal absorption results at 15 K by Martin and co-workers. The possible presence of a Jahn-Teller effect for the $\Gamma_1(^1A_{1g}) \rightarrow \Gamma_5(^1E_g)$ transition for $PdBr_4^{2-}$ in Cs_2ZrBr_6 has been examined. A Cotton–Harris molecular orbital calculation has been carried out for $PdCl_4^{2-}$ and $PdBr_4^{2-}$ ions. The MO results have been used in conjunction with a crystal field calculation to correlate the available experimental data for these two ions.

I. Introduction

Polarized crystal spectra for the tetrachloropalladate(II) ion at liquid helium temperature have been reported by Francke and Moncuit.[1] Also, Rush, Martin, and LeGrand[2] have reported liquid helium polarized crystal spectra for the tetrachloropalladate(II) ion and the tetrabromopalladate(II) ion. Similar measurements have been carried out for the corresponding platinum(II) salts.[3,4]

We have reported experiments[5–7] where we have doped both the $PtCl_4^{2-}$ and the $PdCl_4^{2-}$ ions as substitutional impurities in cubic antifluorite hosts of the Cs_2ZrCl_6 type and observed the optical spectra at 4.2 and 2 K, respectively. In this type

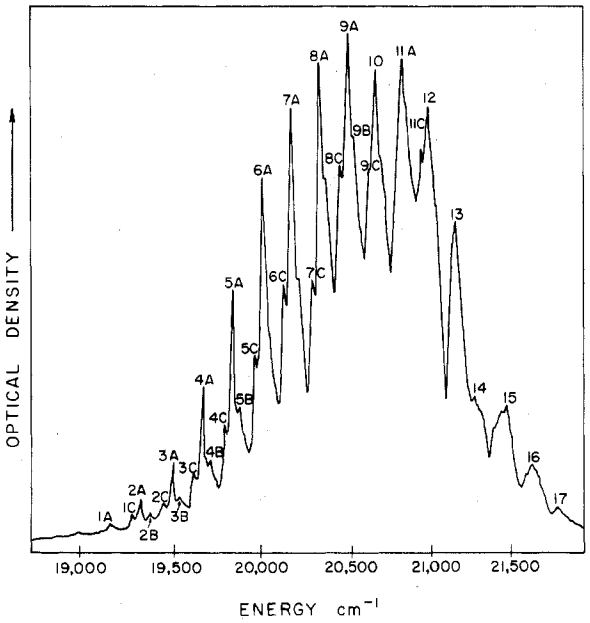

Figure 1. Microphotometer tracing of bands 1 and 2 for Cs_2PdBr_4 in Cs_2ZrBr_6 at 2 K.

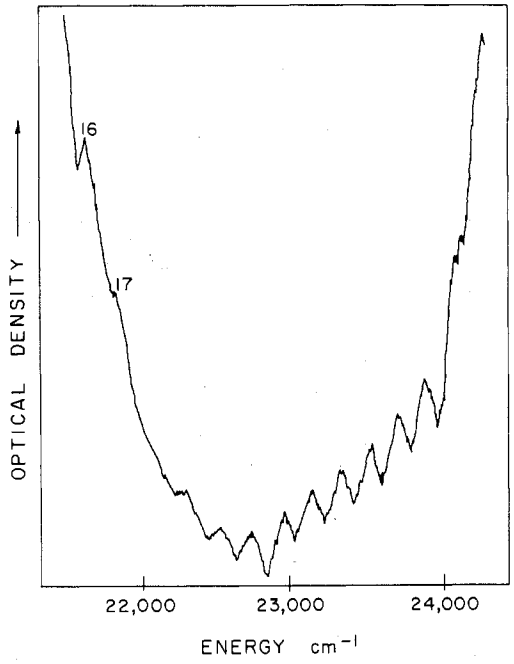

Figure 2. Microphotometer tracing of band 3 for Cs_2PdBr_4 in Cs_2ZrBr_6 at 2 K.

of experiment the MX_4^{2-}–MX_4^{2-} interactions are minimized.

In this paper we report the optical spectra of the tetrabromopalladate(II) ion doped as an impurity in the cesium hexabromozirconate(IV) host lattice at 2 K. For the $\Gamma_1(^1A_{1g}) \rightarrow \Gamma_2(^1A_{2g})$ d–d transition, Martin et al.[2] have observed exceptional vibrational structure for K_2PdBr_4 at 15 K. Comparison of the mixed and pure crystal results will allow us to study the effect of the M–M interactions for one sharply structured transition.

Molecular orbital calculations of the Cotton–Harris type have been carried out for $PdCl_4^{2-}$ and $PdBr_4^{2-}$. The results are in reasonable agreement with the experimental data. Also, crystal field calculations for $PtCl_4^{2-}$ and $PtBr_4^{2-}$ have been used to predict the optical spectra of $PdBr_4^{2-}$ from the results for $PdCl_4^{2-}$. Thus, crystal field and molecular orbital results have been used to compare the $PdCl_4^{2-}$ vs. $PdBr_4^{2-}$ systems and the corresponding platinum systems.

II. Experimental Section

The K_2PdBr_4 used for preparation of the Cs_2PdBr_4 was purchased from D. F. Goldsmith Chemical and Metal Corp. The Cs_2PdBr_4 was prepared by adding a stoichiometric amount of CsBr to a saturated solution of K_2PdBr_4 in about 6 M HBr. K_2PdBr_4 hydrolyzes rapidly in water but the presence of HBr prevents this. Cs_2PdBr_4 is much less soluble than K_2PdBr_4 and precipitates readily as a reddish powder.

The procedure for preparing and growing the mixed Cs_2ZrBr_6 crystals has been described in an earlier publication.[8] Also, the techniques for recording the mixed crystal optical spectra have been described previously.[5,7]

Analysis of the amount of Cs_2PdBr_4 doped in the Cs_2PdBr_4–Cs_2ZrBr_6 mixed crystals was determined by atomic absorption spectroscopy as described previously[7] for mixed Cs_2PdCl_4–Cs_2ZrCl_6 type crystals. The mole percent of Cs_2PdBr_4 in these mixed crystals was about 0.5%.

The extinction coefficient of the $PdBr_4^{2-}$ ion doped in Cs_2ZrBr_6 at liquid helium temperature was determined by measuring the absorbance of the mixed crystal on a Cary 14 spectrophotometer. The concentration of Cs_2PdBr_4 in the mixed crystal was calculated from the unit cell length of Cs_2ZrBr_6[9] and from the mole percent of Cs_2PdBr_4 in the mixed crystal. The crystal thickness was determined to be 1.37 mm. Using the Beer–Lambert law and relationship 1 values

$$f = 4.32 \times 10^{-9} \int \epsilon(\bar{\nu})\, d\bar{\nu} \qquad (1)$$

of the extinction coefficients, ϵ, and oscillator strengths, f, were obtained.

III. Results

Five bands were observed in the absorption spectrum of Cs_2PdBr_4–Cs_2ZrBr_6 mixed crystals at liquid helium temperature. Band 1 occurs as a progression in three peaks from 19 185 to 21 836 cm^{-1} and is shown in Figure 1. It is very similar in appearance to the band assigned as $\Gamma_1(^1A_{1g}) \rightarrow \Gamma_2(^1A_{2g})$ for $PdCl_4^{2-}$ and has about the same relative intensity. Band 2 corresponds to a hump under band 1, as shown in Figure 1, which begins at 19 500 cm^{-1} and continues to 21 800 cm^{-1}. Band 3, as shown in Figure 2, appears as a low intensity progression in a single peak from 22 700 to 23 900 cm^{-1}.

Above 25 000 cm^{-1} no detailed vibronic structure is evident. However, two strong and broad peaks have been observed with maxima at about 27 000 and 30 000 cm^{-1}.

The absorbance of a single Cs_2PdBr_4–Cs_2ZrBr_6 crystal was kindly measured by Professor D. Martin with a Cary spectrophotometer at room temperature and at 16 K. At 20 200 cm^{-1} the extinction coefficient of the mixed crystal system was determined to be 140 at room temperature and 76 at 16 K. In comparison, Martin[2] has found the extinction coefficient of a pure K_2PdBr_4 crystal at 300 and 15 K to be ~300 and ~120, respectively. Thus, for the $\Gamma_1(^1A_{1g}) \rightarrow \Gamma_2(^1A_{2g})$ transition at 16 K the extinction coefficients and the oscillator strength in the mixed crystal system are reduced by about 35% from the pure crystal case. This reduction in intensity could be partly due to the variation in cation from Cs^+ to K^+ and partly due to a difference in the index of refraction of the two systems. Martin and co-workers[2] have reported $n_O = 1.75$ and $n_E = 1.58$ for K_2PdBr_4 at Na D wavelength while we have found the refractive index of the host crystal Cs_2ZrBr_6 to be about 5% lower than the average value of K_2PdBr_4 at the same wavelength. At the wavelengths near the absorption band one would predict[10] the index of refraction of the pure crystal to be higher than that of the mixed crystal. Since the oscillator strength is proportional to the index of refraction, this should be partially responsible for the observed difference in the oscillator strengths.

IV. Molecular Orbital Calculation

Molecular orbital calculations are extremely useful in attempting to assign the observed electronic transitions in a molecule. One common calculation which is relatively simple

Table I. Values of the H_{ii} Matrix Elements for the $PdCl_4^{2-}$ and $PdBr_4^{2-}$ Molecular Orbital Calculations[a]

Orbital	H_{ii} for $PdCl_4^{2-}$, eV	H_{ii} for $PdBr_4^{2-}$, eV
5s(M)	−8.99	−8.99
$5p_x,5p_y,5p_z$(M)	−4.41	−4.41
$4d_{xy},4d_{xz},4d_{yz},4d_{x^2-y^2},4d_{z^2}$(M)	−11.16	−11.16
3s(L)	−24.00	−23.76
$3p_x,3p_y,3p_z$(L)	−15.10	−15.55

[a] (M) indicates a palladium orbital while (L) is for the ligand orbitals. The atomic coordinates of the orbitals are the same as in ref 11.

to do is an extended-Hückel (EH) molecular orbital calculation of the Cotton–Harris type.[11] This is the type of calculation we have carried out.

The assumptions underlying the EH model are as follows. First, the molecular orbitals are linear combinations of the atomic orbitals (LCAO approximation). Second, the overlap integrals do not change appreciably with the variation of the charge distribution during the course of the calculation. This assumption eliminates the need to recalculate the overlap integrals at every stage of the calculation. Third, the diagonal elements of the Hamiltonian matrix, H_{ii}, vary with charge distribution according to a predetermined ratio. This ratio has been fixed as 1 eV/unit charge by Cotton and Harris in order to fit the observed optical transitions of $PtCl_4^{2-}$. Fourth, the off-diagonal Hamiltonian matrix elements can be computed by the Mulliken–Wolfsberg–Helmholtz approximation

$$H_{ij} = KS_{ij}(H_{ii} + H_{jj})/2 \tag{2}$$

where S_{ij} is the overlap matrix element. K has been varied by Cotton and Harris for $PtCl_4^{2-}$ and they found the most reasonable value for K to be in the range of 1.7 to 1.8.

Calculation of the Diagonal Elements of the Hamiltonian Matrix, H_{ii}, for $PdCl_4^{2-}$ and $PdBr_4^{2-}$. The diagonal Hamiltonian matrix elements have been calculated for $PdCl_4^{2-}$ and $PdBr_4^{2-}$ by the Cotton and Harris procedure of expressing the diagonal matrix elements, H_{ii}, as the free ion part, A_{ii}, plus a correction factor. The A_{ii}'s for the palladium orbitals were determined from the ionization potentials for $Pd^0 \rightarrow Pd^+ + e^-$. The following processes were considered:

5s $4d^95s \rightarrow 4d^9 + e$
$4d^85s^2 \rightarrow 4d^85s + e$
$4d^85s5p \rightarrow 4d^85p + e$
5p $4d^95p \rightarrow 4d^9 + e$
$4d^85s5p \rightarrow 4d^85s + e$
4d $4d^{10} \rightarrow 4d^9 + e$
$4d^95s \rightarrow 4d^85s + e$
$4d^95p \rightarrow 4d^85p + e$

The energies of the states in Pd^0 and Pd^+ were obtained by multiplet averaging of the energies of the individual states found in Moore's tables.[12] The energy difference between the two states was then calculated, and once the energies of all the processes had been found, the energies were averaged. The H_{ii}'s for Pd^0 are listed in Table I. The values for the H_{ii}'s of the $Cl^{-1/2}$ valence orbitals are taken from Cotton and Harris. Also, the H_{ii}'s for $Br^{-1/2}$ are given in Table I. Note that the H_{ii}'s are negative because energy must be added to the orbital to remove an electron from it.

Calculation of the Overlap Matrix Elements, S_{ij}. A Slater-type orbital is a wave function of the form

$$\psi = N^{1/2}r^n e^{-\alpha r}Y(\theta,\phi) \tag{3}$$

where $N^{1/2}$ is the appropriate radial normalization factor, α is a constant, and $Y(\theta,\phi)$ is the appropriate normalized spherical harmonic function. In order to simplify the calculation of the overlap matrix elements, it was assumed that the atomic orbitals of interest can be expressed as a linear combination of Slater-type orbitals (LCSTO's)

$$\psi = \sum_i C_i N_i^{1/2} r^{n_i} e^{-\alpha_i r} Y(\theta,\phi) \tag{4}$$

Harrison has written a computer program, EXPFIT, which will fit a linear combination of exponentials to a set of data either generated by input analytical functions or fed directly into the program. The program constructs a set of evenly spaced values of r and either calculates the value of the wave function at that distance (for the function option) or interpolates between the two nearest input values of the radius (for the numerical data option). The program then solves for the α_i's by Prony's method.[13] After determining the set of α_i's for each exponent, the program then determines the coefficients by a least-squares method. Once the LCSTO's have been found, the overlap elements can be evaluated using computer programs already written by other workers.

The Pd^0 4d, 5s, and 5p wave functions were calculated by a Hartree–Fock–Slater self-consistent field program written by Herman and Skillman.[14] The numerical wave functions that are generated have the correct number of radial nodes, are normalized, and are continuous. These particular numerical wave functions have been used by Lea[15] to calculate coherent Hartree–Fock–Slater atomic x-ray scattering factors for neutral atoms, an application which would seem to require good wave functions. This suggests that we may have some confidence in the wave functions we are using.

Since the HFSSCF program will not generate numerical wave functions for unoccupied orbitals and the ground state of Pd^0 is $4d^{10}$, calculations also had to be done on excited states of Pd^0 in order that wave functions for the 5s and 5p orbitals of palladium might be generated. The ground state and three excited states of Pd^0 were calculated using this program. The numerical wave functions generated for each state were then fit to a LCSTO's and the function which had the best fit was taken as the function for the particular orbital. While it is recognized that HFSSCF calculations are strictly applicable only to the ground state, it was thought that this would give a good representation of the wave function, since we were not interested in the energy. This is borne out by our fitting calculations, since the functions calculated for different electronic configurations agreed to three significant figures in the exponents α_i and were within an average of 15% in the coefficients.

The wave functions for palladium were for Pd^0. In order to have the charge on the $PdCl_4^{2-}$ complex come out correctly, it was necessary to use $Cl^{-1/2}$ rather than Cl^{-1} or Cl^0 wave functions. The initial charge on the palladium was chosen as zero because the charge on platinum in Cotton and Harris' $PtCl_4^{2-}$ calculation was +0.439, which is closer to zero than it is to one. The numerical $Cl^{-1/2}$ functions were a numerical average of the Cl^0 and Cl^{-1} functions. The $PdBr_4^{2-}$ complex was treated in the same fashion as the $PdCl_4^{2-}$ complex.

Molecular Orbital Results for $PdCl_4^{2-}$ and $PdBr_4^{2-}$ Ions. Once the diagonal and off-diagonal matrix elements of the secular equation

$$|H_{ij} - ES_{ij}| = 0 \tag{5}$$

have been calculated, a computer program was used to solve the secular equation for the eigenvalues and eigenfunctions. A self-consistent charge calculation was performed and convergence occurred in 13 iterations. The symmetries of the calculated molecular orbitals, their energies, and the major components of the eigenfunctions for $PdCl_4^{2-}$ and $PdBr_4^{2-}$ are listed in Table II.

It can be seen from Table II that the ordering of the molecular orbitals for $PdCl_4^{2-}$ is almost the same as that reported for $PtCl_4^{2-}$ by Cotton and Harris, except that the

Table II. Eigenvalues, Components of the Eigenvectors,[a] and Symmetries of Molecular Orbitals for $PdCl_4^{2-}$ and $PdBr_4^{2-}$ Ions

Orbital	Major components of eigenvectors	Symmetry	Energy, eV $PdCl_4^{2-}$	Energy, eV $PdBr_4^{2-}$
1, 2	5p, *n*s, *n*p	e_u	10.73	11.74
3	5s, *n*p, *n*s, $4d_{z^2}$	a_{1g}	7.69	1.33
4	5p, *n*p	a_{2u}	−1.50	−.34
5	$4d_{x^2-y^2}$, *n*p, *n*s	b_{1g}	−8.85	−9.29
6	$4d_{xy}$, *n*p	b_{2g}	−11.37	−11.54
7, 8	$4d_{xz}$, $4d_{yz}$, *n*p	e_g	−11.46	−11.58
9	$4d_{z^2}$, 5s, *n*p, *n*s	a_{1g}	−11.73	−11.72
10	*n*p	a_{2g}	−12.80	−12.65
11, 12	*n*p, 5p, *n*s	e_u	−13.25	−13.44
13	*n*p	b_{2u}	−13.95	−14.05
14	*n*p, $4d_{x^2-y^2}$	b_{1g}	−14.25	−14.24
15, 16	*n*p, $4d_{xz}$, $4d_{yz}$	e_g	−14.63	−14.95
17	*n*p, 5p	a_{2u}	−15.03	−15.84
18, 19	*n*p, *n*s, 5p	e_u	−15.18	−15.51
20	*n*p, $4d_{xy}$	b_{2g}	−15.87	−16.51
21	*n*p, 5s, *n*s, $4d_{z^2}$	a_{1g}	−16.01	−17.07
22	*n*s, $4d_{x^2-y^2}$, *n*p	b_{1g}	−23.07	−22.74
23, 24	*n*s, 5p, *n*p	e_u	−23.44	−23.26
25	*n*s, 5s, $4d_{z^2}$, *n*p	a_{1g}	−24.23	−23.78

[a] For the chloride ligand $n = 3$ and for the bromide ligand $n = 4$.

$b_{1g}(2)$ (No. 14) state is higher in energy in $PdCl_4^{2-}$ than $a_{2u}(1)$ (No. 17) and $e_g(1)$ (No. 15 and 16) states, whereas in $PtCl_4^{2-}$ it is lower in energy than each of these. There are also differences in ordering from that reported by Basch and Gray[16] in their calculation for $PdCl_4^{2-}$, although the ordering of the d orbitals is the same.

A list of the lowest energy, spin allowed transitions in $PdCl_4^{2-}$ (and $PdBr_4^{2-}$) from our calculation and the Xα calculation of Messmer, Interrante, and Johnson[17] is found in Table III. Our molecular orbital results agree better with the accepted assignments of the low energy bands than the Xα molecular results. However, the Xα model gives better results for the observed charge transfer transitions.

V. Assignment of Experimental Data

Crystal Field Model for Assignment of Low-Energy Transitions. The crystal field model used in this work has been discussed in two previous publications[5,7] on $PtCl_4^{2-}$ and $PdCl_4^{2-}$. The ion $PdBr_4^{2-}$ possesses D_{4h} symmetry. When Pd^{2+} is placed in a strong crystal field the $4d^8$ orbitals will have an energy level scheme as follows:

$$b_{1g}(d_{x^2-y^2}) > b_{2g}(d_{xy}) > e_g(d_{xz},d_{yz}) > a_{1g}(d_{z^2})$$

The matrix elements which describe the crystal field, the interelectronic repulsion, and the spin–orbit interaction have been given by Fenske, Martin, and Ruedenberg.[18] F_2 and F_4 are the Slater–Condon parameters, λ is the spin–orbit interaction parameter, and Δ_1, Δ_2, Δ_3 are the strong field parameters: $\Delta_1 = d_{x^2-y^2} - d_{xy}$, $\Delta_2 = d_{x^2-y^2} - d_{z^2}$, $\Delta_3 = d_{x^2-y^2} - d_{xz}, d_{yz}$.

To assign the low energy observed bands for $PdBr_4^{2-}$ in terms of a crystal field model, we first calculated the change of the six parameters in going from $PtCl_4^{2-}$ to $PtBr_4^{2-}$ and then assumed the same variation to predict the changes in the spectra from $PdCl_4^{2-}$ to $PdBr_4^{2-}$. The first step of the analysis involved finding suitable values of the crystal field parameters for $PtBr_4^{2-}$. Using the values of the parameters for $PtCl_4^{2-}$ given by Patterson, Godfrey, and Khan[5] and the experimental data for $PtBr_4^{2-}$ for the singlet–singlet absorptions reported by Kroening, Rush, Martin, and Clardy,[4] a least-squares fit was made by varying only Δ_1, Δ_2, Δ_3 and a new set of parameters was obtained. Next, F_2, F_4, and λ were varied, with Δ_1, Δ_2, Δ_3 held constant, to obtain the best fit to the experimental energies. Then, F_2, F_4, and λ were held constant and Δ_1, Δ_2, Δ_3 were varied to give the best fit to the data.

In the second stage of the crystal field analysis the percentage change in each crystal field parameter was calculated for $PtCl_4^{2-}$ vs. $PtBr_4^{2-}$. These same percent variations were then applied to the crystal field parameters for $PdCl_4^{2-}$ given by HPG,[7] and a set of approximate excited state energies for $PdBr_4^{2-}$ was obtained. A further refinement of these values was then carried out with a least-squares technique to fit the observed values for K_2PdBr_4 at 15 K given by Rush, Martin, and LeGrand. A summary of the crystal field calculations is given in Table IV.

Our assignments of the d–d transitions for $PdBr_4^{2-}$ agree with the assignments given by RML in most cases. The assignment of the band at 15 700 cm^{-1} as the $\Gamma_1(^1A_{1g}) \rightarrow \Gamma_5,\Gamma_1(^3A_{2g})$ transition agrees with the polarization selection rules since this transition should appear in both *xy* and *z* polarizations and experimentally this is the case for the K_2PdBr_4 crystal system. By the same token the transition $\Gamma_1(^1A_{1g}) \rightarrow \Gamma_2(^1A_{2g})$ is expected to appear only in *xy* polarization and has been assigned to the 20 200 cm^{-1} (*xy*) transition by RML. Band 1 with a maximum of about 20 200 cm^{-1} for the Cs_2PdBr_4–Cs_2ZrBr_6 system has also been assigned to the $\Gamma_1(^1A_{1g}) \rightarrow \Gamma_2(^1A_{2g})$ transition.

The 17 400 and 26 990 cm^{-1} observed bands of RML have been assigned to the $\Gamma_1(^1A_{1g}) \rightarrow \Gamma_4(^3B_{1g})$ and the $\Gamma_1(^1A_{1g}) \rightarrow \Gamma_3(^1B_{1g})$ transitions respectively, since their relative oscillator strengths are in reasonable agreement with our calculated relative intensities. The 26 990 cm^{-1} observed band is not assigned to a spin-forbidden charge transfer band because the appreciable spin–orbit interaction for bromine should result in a transition with an extinction coefficient greater than 21.

From MCD studies of $PdBr_4^{2-}$ in solution at room temperature, Schatz and co-workers[19] have reported an *A* term for a band at 19 600 cm^{-1} and they have assigned this band as the $\Gamma_1(^1A_{1g}) \rightarrow \Gamma_5(^1E_g)$ transition. The same assignment

Table III. Comparison of MO Extended-Hückel (EH) and Xα Calculated Transition Energies with Experimental Data

Type	Excited state	Calcd energy, cm^{-1}, for $PdCl_4^{2-}$ (Xα)[d]	Calcd energy, cm^{-1}, for $PdCl_4^{2-}$ (EH)[c]	Exptl energy, cm^{-1}, for $PdCl_4^{2-}$	Calcd energy, cm^{-1}, for $PdBr_4^{2-}$ (EH)[c]	Exptl energy, cm^{-1}, for $PdBr_4^{2-}$
d–d	$^1A_{2g}$	28 000	20 300	21 454[a]	18 150	20 200[b]
d–d	^1E_g	28 000	21 100	22 530[a]	18 470	21 977[b]
d–d	$^1B_{1g}$	35 000	23 200	28 909[a]	19 600	
CT L–M	$^1B_{2g}$		31 900		27 100	
CT L–M	^1E_u	35 000	35 500	35 720[b]	33 500	30 200[b]
CT L–M	$^1A_{2u}$	37 000	41 100	37 400[b]	38 400	30 900[b]
CT L–M	$^1A_{1g}$		43 600		39 900	
CT L–M	^1E_g		46 600		45 700	
CT L–M	^1E_u	44 000	51 100	44 980[b]	50 200	40 000[b]

[a] Harrison, Patterson, and Godfrey, ref 7. [b] Rush, Martin, and LeGrand, ref 2. [c] This calculation. [d] Messmer, Interrante, and Johnson, ref 17.

Table IV. Summary of Crystal Field Results for PtX_4^{2-} and PdX_4^{2-} where X = Cl, Br

State	Energy calcd,[a] cm^{-1}, for $PtBr_4^{2-}$	Energy obsd,[b] cm^{-1}, for $PtBr_4^{2-}$	Extinction coeff ϵ_{exptl}[b]	Rel[c] intensity calcd
$\Gamma_1(^1A_{1g})$	0			
$\Gamma_1(^3E_g)$	14 665			2.5
$\Gamma_2(^3E_g)$	14 821			4.1
$\Gamma_5(^3E_g)$	15 546			2.7
$\Gamma_4(^3E_g)$	16 482			2.2
$\Gamma_3(^3E_g)$	17 016	16 900 (*z*), 17 000 (*xy*)	1 (*z*), 4 (*xy*)	3.4
$\Gamma_5(^3A_{2g})$	19 027	18 800 (*z*), 19 100 (*xy*)	12 (*z*), 15 (*xy*)	3.1
$\Gamma_1(^3A_{2g})$	19 340			4.3
$\Gamma_5(^3B_{1g})$	22 538	22 600 (*z*), 22 700 (*xy*)	3 (*z*), 13 (*xy*)	13.2
$\Gamma_4(^3B_{1g})$	23 322			2.4
$\Gamma_2(^1A_{2g})$	24 069	24 400 (*xy*)	46	95.5
$\Gamma_5(^1E_g)$	26 937	27 400 (*z*), 26 800 (*xy*)	44 (*z*), 73 (*xy*)	83.9
$\Gamma_3(^1B_{1g})$	34 080	33 800 (*z*)	39	94.9

	Energy calcd, cm^{-1}, for $PdBr_4^{2-}$, extrap tech[d]	Energy calcd, cm^{-1}, for $PdBr_4^{2-}$, LS tech[e]	Energy[f] obsd, cm^{-1}, for $PdBr_4^{2-}$	Extinction coeff ϵ_{exptl}[f]	Rel intensity calcd[c,g]
$\Gamma_1(^1A_{1g})$	0	0			
$\Gamma_1(^3E_g)$	10 316	11 974			1.7
$\Gamma_2(^3E_g)$	10 380	12 053			2.3
$\Gamma_5(^3E_g)$	11 060	12 522			1.6
$\Gamma_4(^3E_g)$	11 844	13 070			1.4
$\Gamma_3(^3E_g)$	12 253	13 426			2.2
$\Gamma_5(^3A_{2g})$	15 254	15 530			2.0
$\Gamma_1(^3A_{2g})$	15 561	15 701	15 700 (*z*)	<1	2.6
$\Gamma_5(^3B_{1g})$	17 409	17 058	16 960 (*xy*)	4.8	4.9
$\Gamma_4(^3B_{1g})$	18 434	17 500	17 400 (*z*)	<1	1.5
$\Gamma_2(^1A_{2g})$	19 822	20 228	20 200 (*xy*)	177	97.4
$\Gamma_5(^1E_g)$	20 526	22 006	21 730 (*z*), 22 100 (*xy*)	33 (*z*), 31 (*xy*)	93.3
$\Gamma_3(^1B_{1g})$	27 041	27 018	26 990 (*z*)	25	96.8

[a] Energy calculated for the parameters $F_2 = 1305\ cm^{-1}$, $F_4 = 52\ cm^{-1}$, λ 816 cm^{-1}, $\Delta_1 = 24\,217\ cm^{-1}$, $\Delta_2 = 39\,164\ cm^{-1}$, $\Delta_3 = 30\,463\ cm^{-1}$. The rms deviation between the calculated and observed values is 241 cm^{-1}. [b] R. F. Kroening, R. M. Rush, D. S. Martin, Jr., and J. C. Clardy, *Inorg. Chem.*, **13**, 1366 (1974). [c] The relative intensities were calculated by means of a spin intensity formula given by Schroeder (*J. Chem. Phys.*, **37**, 2553 (1963)). With this formula a pure singlet–singlet transition has a relative intensity of 100, while a pure singlet–triplet transition has a relative intensity of 0. [d] Energy calculated for parameters $F_2 = 1022\ cm^{-1}$, $F_4 = 48\ cm^{-1}$, λ 725 cm^{-1}, $\Delta_1 = 20\,051\ cm^{-1}$, $\Delta_2 = 31\,009\ cm^{-1}$, $\Delta_3 = 22\,946\ cm^{-1}$. The rms deviation between the calculated and observed values is 768 cm^{-1}. [e] Energy calculated for parameters $F_2 = 1105\ cm^{-1}$, $F_4 = 51\ cm^{-1}$, λ 520 cm^{-1}, $\Delta_1 = 20\,715\ cm^{-1}$, $\Delta_2 = 31\,408\ cm^{-1}$, $\Delta_3 = 25\,377\ cm^{-1}$ with rms deviation = 77 cm^{-1}. [f] R. M. Rush, D. S. Martin, Jr., and R. G. LeGrand, *Inorg. Chem.*, **14**, 2543 (1975). [g] From the least-squares technique.

has been given to the 21 730 cm^{-1} (*z* polarization) and 22 100 cm^{-1} (*xy* polarization) bands by Martin and co-workers in their study of single K_2PdBr_4 crystals at 15 K. This represents a difference in energy of about 2400 cm^{-1}. Our bands labeled 2 and 3 have maxima at 20 600 and 23 200 cm^{-1}, respectively, and lie in the energy range of the $\Gamma_1(^1A_{1g}) \rightarrow \Gamma_5(^1E_g)$ band (19 000–24 000 cm^{-1}) for single crystals as reported by Martin at 15 K. Two types of assignments are reasonable to the authors. First, if the *xy* and *z* polarization data for this transition are averaged one gets an energy of 21 915 cm^{-1} in contrast to an average energy of 21 900 cm^{-1} for bands 2 and 3 in the mixed crystals. Thus, it is possible that bands 2 and 3 are just the beginning and end, respectively, of the $^1A_{1g} \rightarrow {}^1E_g$ transition. Further, since Martin's data indicate that the $\Gamma_1(^1A_{1g}) \rightarrow \Gamma_2(^1A_{2g})$ band is over five times more intense than the $\Gamma_1(^1A_{1g}) \rightarrow \Gamma_5(^1E_g)$ band, it must be true that the hump labeled as band 2 is mostly the $\Gamma_1(^1A_{1g}) \rightarrow \Gamma_2(^1A_{2g})$ band.

A second possible assignment for bands 2 and 3 to consider is that they represent the $\Gamma_1(^1A_{1g}) \rightarrow \Gamma_5(^1E_g)$ transition with a Jahn–Teller effect present. Ballhausen[20] has considered Jahn–Teller instability in square-planar complexes in the presence of spin–orbit coupling. If the spin–orbit value calculated from the crystal field model, and the ground state b_{1g} and b_{2g} vibrational mode energies, and a range of JT strengths are used in the Ballhausen mathematical model the predicted JT electronic spectrum is in reasonable agreement with the mixed crystal bands 2 and 3 spectra only in the strong static case where the JT splitting is about 2600 cm^{-1}. For smaller values of the JT energy, the predicted spectrum shows irregularities which are not present in the experimental spectrum. One way to test these two possible assignments for bands 2 and 3 is to measure the MCD spectrum at 2 K. If assignment I is correct, bands 2 and 3 should both show an *A* term of about the magnitude observed by Schatz and co-workers for $PdBr_4^{2-}$ in solution. Experiments of this type are to be carried out with Professor O. Weigang of this department in the near future.

Molecular Orbital Model for Assignment of Non-d–d Transitions. Our Cotton–Harris type of molecular orbital calculations predict (Table III) for $PdCl_4^{2-}$ that the $^1A_{1g} \rightarrow {}^1E_{u(1)}$, $^1A_{2u}$, and $^1E_{u(2)}$ transitions occur at 35 500, 41 100, and 51 100 cm^{-1}, respectively. We have previously assigned from low-temperature Cs_2PdCl_4–Cs_2ZrCl_6 MCD measurements the $^1A_{1g} \rightarrow {}^1E_{u(1)}$ transition at 35 720 cm^{-1} in good agreement with the MO results. Further, Martin[2] has assigned the $^1A_{1g} \rightarrow {}^1A_{2u}$ transition at 37 400 cm^{-1} from *z*-polarization experiments, in reasonable agreement with the MO results. Also, Martin has assigned the $^1E_{u(2)}$ transition at 45 000 cm^{-1}.

The $^1A_{1g} \rightarrow {}^1B_{2g}$, $^1A_{1g}$, ^1E_g parity-forbidden charge-transfer transitions predicted to be at 31 900, 43 600, and 46 600 cm^{-1}, respectively, are expected to be much weaker than the broad parity allowed transitions. Also they lie in an energy region predicted where the stronger parity-allowed transitions occur; thus, it is not surprising they have not been observed. For example, at 31 900 cm^{-1}, where the $^1A_{1g} \rightarrow {}^1B_{2g}$ transition is predicted to occur in *xy* polarization by virtue of e_u internal vibrational modes, the $^1A_{1g} \rightarrow {}^1E_u$ band is present with appreciable intensity.

For $PdBr_4^{2-}$ the $^1A_{1g} \rightarrow {}^1E_{u(1)}$, $^1A_{2u}$, and $^1E_{u(2)}$ transitions are predicted to be at 33 500, 38 400, and 50 200 cm^{-1}, re-

spectively. From polarization measurements with K_2PdBr_4, Martin has assigned these bands to be at 30 200, 30 900, and 40 000 cm^{-1}, respectively. The two ^1E_u bands follow the same trend in the chloride and bromide salts. However, the $^1A_{2u}$ band in the bromide salt is not in good agreement with the MO results in contrast to the $PdCl_4^{2-}$ results. Also, in the mixed crystal system we have observed a band at 27 000 cm^{-1}, and Martin has observed bands at 26 990, 36 500, 37 000, and 43 200 cm^{-1}.

The additional bands observed by Martin at 26 990 and 36 500 cm^{-1} have extinction coefficients of 3700 and 5400 cm^{-1} M^{-1}, respectively. These large extinction coefficients indicate that the parity-forbidden $^1A_{1g} \rightarrow {}^1B_{2g}$, $^1A_{1g}$, and ^1E_g bands are not responsible, and the effects of spin–orbit interaction must be considered. The much larger spin–orbit coupling parameter[21] for the Br atom (2457 cm^{-1}) in contrast to the Cl atom (587 cm^{-1}) should give rise to considerable intensity borrowing for the spin triplet states from the singlet states.

In the presence of spin–orbit interaction, a ^3Eu state gives rise to Γ_{1u}, Γ_{2u}, Γ_{3u}, Γ_{4u}, and Γ_{5u} states, with transitions from the Γ_{1g} ground state to the Γ_{2u} and Γ_{5u} states only allowed by symmetry. Let us consider only the coupling between the $\Gamma_5(^1Eu)$ and $\Gamma_5(^3Eu)$ states because of spin–orbit interaction. If Δ denotes the splitting between the two states because of electronic repulsion in the absence of spin–orbit coupling, then it is easy to show by standard methods[22] that with spin–orbit coupling the mixing of the singlet and triplet states is given by the secular determinant

$$\begin{vmatrix} (\Delta - E) & i\lambda_{Br}/2 \\ -i\lambda_{Br}/2 & (-E) \end{vmatrix} = 0 \qquad (6)$$

where λ_{Br} is the spin–orbit interaction of the bromine atom. If this eq 6 is used for the $\Gamma_5(^1Eu)$ state at 30 200 cm^{-1} and the $\Gamma_5(^3Eu)$ state at 26 990 cm^{-1}, with λ_{Br} 2457 cm^{-1}, then Δ is calculated to be 2200 cm^{-1}. The $\Gamma_5(^3Eu)$ state has 16.7% singlet character with a predicted extinction coefficient of 2130. If the λ_{Br} and Δ values of 2457 and 2125 cm^{-1}, respectively, are used for the $\Gamma_5(^1Eu)$ and $\Gamma_5(^3Eu)$ states at 40 000 and 36 500 cm^{-1}, respectively, then the $\Gamma_5(^3Eu)$ state is calculated to have an extinction coefficient of 5790, in contrast to the experimental value of 5400. Thus, we conclude from this simple one-parameter model that it is reasonable to assign the 26 990 and 36 500 cm^{-1} bands to spin-forbidden charge transfer transitions because of the bromine spin–orbit interaction.

Assignment of Vibronic Structure for d–d Transition. In the Cs_2PdBr_4–Cs_2ZrBr_6 mixed crystal system, vibronic structure for the $\Gamma_1(^1A_{1g}) \rightarrow \Gamma_2(^1A_{2g})$ transition is observed as a progression of three peaks. The energy range is from 19 185 to 21 836 cm^{-1} (Table V). It has been previously shown that for a transition of this type there are two molecular e_u vibrations which may mix with the final electronic state to give an allowed vibronic transition. The two vibrations are ν_6, the asymmetric stretch mode, and ν_7, an in-plane bending mode. As shown in Table V, the average spacing between A peaks is 166 cm^{-1}, the average spacing between B and C peaks is 87 cm^{-1}, and the average spacing between C and A peaks is 45 cm^{-1}. The spacing of 166 cm^{-1} represents the frequency of the a_{1g} vibrational mode in the $\Gamma_1(^1A_{1g})$ excited state. This is about 14% lower than the value of 187–192 cm^{-1} of $\nu_1(a_{1g})$ for the ground state as obtained by Raman spectroscopy.[23–25]

Martin and co-workers have also found vibronic structure for the $\Gamma_1(^1A_{1g}) \rightarrow \Gamma_2(^1A_{2g})$ transition in their study of a K_2PdBr_4 single crystal at 15 K. Their spectrum shows groups of four components which appear as a progression. They have assigned the two strong peaks as ν_6 and ν_7 and the weak ones as the lattice mode vibration and a combination mode. They have suggested that ν_7 may be slightly larger than its value of 140 cm^{-1} in the ground state. The differences between ν_6–ν_7 and ν_6–ν_L are 50 and 123 cm^{-1}, respectively.

Table V. Assignment of Vibronic Peaks for the $\Gamma_1(^1A_{1g}) \rightarrow \Gamma_2(^1A_{2g})$ Transition for $PdBr_4^{2-}$ in Cs_2ZrBr_6 at 2 K

Peak No.	Energy, cm^{-1}	Excited state assignment I
1A	19 184.5	$\Gamma_2(^1A_{2g}) + \nu_6$
1C	19 297.0	$+ \nu_7 + \nu_1$
2A	19 350.8	$+ \nu_6 + \nu_1$
2B	19 392.1	$+ \nu_L + 2\nu_1$
2C	19 481.7	$+ \nu_7 + 2\nu_1$
3A	19 530.0	$+ \nu_6 + 2\nu_1$
3B	19 570.9	$+ \nu_L + 3\nu_1$
3C	19 639.0	$+ \nu_7 + 3\nu_1$
4A	19 683.8	$+ \nu_6 + 3\nu_1$
4B	19 717.6	$+ \nu_L + 4\nu_1$
4C	19 804.3	$+ \nu_7 + 4\nu_1$
5A	19 851.1	$+ \nu_6 + 4\nu_1$
5B	19 883.5	$+ \nu_L + 5\nu_1$
5C	19 970.9	$+ \nu_7 + 5\nu_1$
6A	20 016.0	$+ \nu_6 + 5\nu_1$
$6B_1$	20 045.3	$+ \nu_L' + 6\nu_1$
$6B_2$	20 068.3	$+ \nu_L'' + 6\nu_1$
6C	20 139.0	$+ \nu_7 + 6\nu_1$
7A	20 178.0	$+ \nu_6 + 6\nu_1$
7B	20 211.1	$+ \nu_L + 7\nu_1$
7C	20 303.0	$+ \nu_7 + 7\nu_1$
8A	20 344.8	$+ \nu_6 + 7\nu_1$
$8B_1$	20 372.9	$+ \nu_L' + 8\nu_1$
$8B_2$	20 387.5	$+ \nu_L'' + 8\nu_1$
8C	20 472.2	$+ \nu_7 + 8\nu_1$
9A	20 514.2	$+ \nu_6 + 8\nu_1$
9B	20 545.4	$+ \nu_L + 9\nu_1$
9C	20 640.5	$+ \nu_7 + 9\nu_1$
10A	20 678.5	$+ \nu_6 + 9\nu_1$
10B	20 714.4	$+ \nu_L + 10\nu_1$
10C	20 808.9	$+ \nu_7 + 10\nu_1$
11A	20 842.3	$+ \nu_6 + 10\nu_1$
11C	20 966.9	$+ \nu_7 + 11\nu_1$
12	21 006.5	$+ \nu_6 + 11\nu_1$
13A	21 167.9	$+ \nu_6 + 12\nu_1$
13C	21 288.3	$+ \nu_7 + 13\nu_1$
14A	21 328.7	$+ \nu_6 + 13\nu_1$
14C	21 425.2	$+ \nu_7 + 14\nu_1$
15A	21 498.0	$+ \nu_6 + 14\nu_1$
15C	21 618.4	$+ \nu_7 + 15\nu_1$
16	21 665.7	$+ \nu_6 + 15\nu_1$
17	21 836.1	$+ \nu_6 + 16\nu_1$

For the assignment of the vibronic structure of the $\Gamma_1(^1A_{1g}) \rightarrow \Gamma_2(^1A_{2g})$ transition in our mixed crystal Cs_2PdBr_4–Cs_2ZrBr_6 study there are two possibilities. Alternative I assignment would assign A peaks to ν_6, B peaks to a lattice mode vibration, and C peaks to ν_7. If the value of ν_7 is assumed to be the same as in the ground state,[26] 140 cm^{-1}, then ν_6 is 185 cm^{-1} and ν_L = 53 cm^{-1} for the $^1A_{2g}$ excited state. Comparing this ν_6 value with the ground state value[26] of 260 cm^{-1} shows there is a 29% decrease in ν_6. The ($\nu_6 - \nu_7$) difference of 45 cm^{-1} in the mixed crystal case is very close to the pure K_2PdBr_4 Martin value of 50 cm^{-1}.

The second possible assignment would be to assign the (n + 1) A peaks to ($\nu_6 + n\nu_1$) as before, but now assign the nB peaks to ($\nu_7 + n\nu_1$) and the nC peaks to ($n + 1$)ν_1 plus a lattice mode. This gives a best fit for ν_7 of 125 cm^{-1}, with ν_6 = 257 cm^{-1} and ν_L = 46 cm^{-1}.

We have reported previously a luminescence study of the $OsBr_6^{2-}$ ion doped into Cs_2ZrBr_6[27] in which the energies of the lattice modes observed in the optical luminescence spectrum were determined. This could be done because zero–zero transitions are allowed for this complex by a magnetic dipole mechanism. Three lattice modes were observed with energies of 29, 45, and 59 cm^{-1}. Each of the alternative assignments gives a value for a lattice mode very close to the observed values in the Cs_2OsBr_6–Cs_2ZrBr_6 system.

Alternative assignment I is the same type of assignment made previously for the $PdCl_4^{2-}$ mixed crystal $\Gamma_1(^1A_{1g}) \rightarrow$

$\Gamma_2(^1A_{2g})$ transition where the ν_6 stretch mode has the greatest intensity. However, assignment II gives ν_6 and ν_7 mode energies closer to the ground state values. One way to distinguish between these two assignments is to observe the lowest energy peak. For I the lowest energy $\Gamma_1(^1A_{1g}) \rightarrow \Gamma_2(^1A_{2g})$ peak should be a $B(\nu_L)$ peak while for II the $C(\nu_L)$ peak should appear first. The best spectra now available indicate that alternative I is the most reasonable assignment of the experimental data.

A Franck–Condon analysis of the $\Gamma_1(^1A_{1g}) \rightarrow \Gamma_2(^1A_{2g})$ transition can be carried out to obtain information about the geometry of the $PdBr_4^{2-}$ complex while it is in the $\Gamma_2(^1A_{2g})$ excited electronic state. The details of such a calculation have been described in a previous publication.[5] If the equilibrium internuclear distance of the excited electronic state is greater by a value Δ from the equilibrium internuclear distance of the ground state, the Franck–Condon principle allows the existence of a progression in the symmetric stretch mode. The intensity maximum in the symmetric stretch progression is determined by the ratio of the ground to the excited state vibrational ν_1 frequencies and the value of Δ. Generally, as the value of Δ is increased, the length of the progression increases. The energies and the relative intensities of the $\Gamma_1(^1A_{1g}) \rightarrow \Gamma_2(^1A_{2g})$ transition for the mixed crystal Cs_2PdBr_4–Cs_2ZrBr_6 system were measured and the value of Δ varied until the experimental and theoretical relative intensities matched best. For $PdBr_4^{2-}$, the $\Gamma_2(^1A_{2g})$ excited electronic state is 0.20 Å greater in Pd–Br equilibrium internuclear separation than the $\Gamma_1(^1A_{1g})$ ground state. This is a change of 9% in the equilibrium internuclear separation. This change in equilibrium internuclear separation is relatively insensitive to the baseline choice. For example, if band 2 is considered to be part of band 1, instead of a separate transition, the value of Δ is changed by not more than 0.02 Å. Also, for the same transition in the Cs_2PdCl_4–Cs_2ZrCl_6 system a change of 9% is calculated in the equilibrium internuclear separation.

Finally, it should be noted that the $PdBr_4^{2-}$ $\Gamma_1(^1A_{1g}) \rightarrow \Gamma_2(^1A_{2g})$ spectrum is very similar in vibronic detail, in going from the pure crystal to the mixed crystal case, except for a shift of +625 cm^{-1}. It would seem that this change can be explained best by the variation in cation from K^+ to Cs^+, rather than by the change to a mixed crystal lattice because the cations are nearest neighbors and the $ZrBr_6^{2-}$ ions are next-nearest neighbors to the $PdBr_4^{2-}$ complex.

VI. Summary

It has been shown in this paper that the experimental optical data for the $PdBr_4^{2-}$ and $PdCl_4^{2-}$ complex ions can be reasonably understood on the basis of crystal field and molecular orbital models. Contrasts can be made with the corresponding platinum salts. A comparison of the liquid helium single crystal optical results of Martin for $PdBr_4^{2-}$ and $PdCl_4^{2-}$ and our mixed crystal optical data shows that the electronic absorption maxima change very little in the two cases. Thus, the Pd–Pd interactions in these pure crystal systems correspond to the case of weak metal–metal coupling. The experimental and theoretical techniques described herein can be extended to other Pt and Pd systems. Work is now in progress on materials such as *cis*- and *trans*-dichlorodiammineplatinum(II) where strong metal–metal interactions may occur. These materials are important as possible anticancer drugs.

Acknowledgment. This research was supported in part by the American Cancer Society, Maine. Also, the authors wish to thank Professor D. Martin, Jr., for recording the optical spectra of a Cs_2PdBr_4–Cs_2ZrBr_6 mixed crystal at liquid helium temperature with a Cary spectrophotometer and for his interest in this work.

Registry No. $PdBr_4^{2-}$, 14127-70-9; $PdCl_4^{2-}$, 14349-67-8; $PtBr_4^{2-}$, 14493-01-7; Cs_2ZrBr_6, 36407-58-6.

References and Notes

(1) E. Francke and C. Moncuit, *C. R. Hebd. Seances Acad. Sci., Ser. B*, **271**, 741 (1970).
(2) R. M. Rush, D. S. Martin, Jr., and R. G. LeGrand, *Inorg. Chem.*, **14**, 2543 (1975).
(3) D. S. Martin, Jr., M. A. Tucker, and A. J. Kassman, *Inorg. Chem.*, **4**, 1682 (1965); **5**, 1298 (1966).
(4) R. F. Kroening, R. M. Rush, D. S. Martin, Jr., and J. C. Clardy, *Inorg. Chem.*, **13**, 1366 (1974).
(5) H. H. Patterson, J. J. Godfrey, and S. M. Khan, *Inorg. Chem.*, **11**, 2872 (1972).
(6) H. H. Patterson, T. G. Harrison, and R. G. Belair, *Inorg. Chem.*, **15**, 1461 (1976).
(7) T. G. Harrison, H. H. Patterson, and J. J. Godfrey, *Inorg. Chem.*, **15**, 1291 (1976).
(8) H. H. Patterson, J. L. Nims, and C. M. Valencia, *J. Mol. Spectrosc.*, **42**, 567 (1972).
(9) J. R. Dickinson, S. B. Piepho, J. A. Spencer, and P. M. Schatz, *J. Chem. Phys.*, **56**, 2668 (1972).
(10) (a) S. Glasstone, "Physical Chemistry", 2d ed, Van Nostrand, New York, N.Y., 1946, p 533; (b) O. E. Weigang, Jr., *J. Chem. Phys.*, **41**, 1435 (1964).
(11) F. A. Cotton and C. B. Harris, *Inorg. Chem.*, **6**, 369 (1967).
(12) C. E. Moore, *Natl. Bur. Stand. (U.S.), Circ.*, (1949 and 1952).
(13) F. B. Hildebrand, "Introduction to Numerical Analysis", 2d ed, McGraw-Hill, New York, N.Y., 1974, pp 457–462.
(14) F. Herman and S. Skillman, "Atomic Structure Calculations", Prentice-Hall, Englewood Cliffs, N.J., 1963.
(15) J. D. Lea, Ph.D. Dissertation, University of Texas, 1963.
(16) H. Basch and H. B. Gray, *Inorg. Chem.*, **6**, 365 (1967).
(17) R. P. Messmer, L. V. Interrante, and K. H. Johnson, *J. Am. Chem. Soc.*, **96**, 3874 (1974).
(18) R. F. Fenske, D. S. Martin, Jr., and K. Ruedenberg, *Inorg. Chem.*, **1**, 441 (1962).
(19) A. J. McCaffery, P. N. Schatz, and P. J. Stephens, *J. Am. Chem. Soc.*, **90**, 5730 (1968).
(20) C. J. Ballhausen, *Theor. Chim. Acta*, **3**, 368 (1965).
(21) C. K. Jorgensen, "Absorption Spectra and Chemical Bonding in Complexes", Pergamon Press, Oxford, 1962, p 159.
(22) For example, see S. B. Piepho, P. N. Schatz, and A. J. McCaffery, *J. Am. Chem. Soc.*, **91**, 5994 (1969), or H. Isci and W. R. Mason, *Inorg. Chem.*, **14**, 905 (1975).
(23) P. L. Goggin and J. Mink, *J. Chem. Soc., Dalton Trans.* 1497 (1975), with $\nu_1(a_{1g}) = 188$ cm^{-1}.
(24) P. J. Hendra, *J. Chem. Soc. A*, 1298 (1967), with $\nu_1(a_{1g}) = 192$ cm^{-1}.
(25) J. R. Durig and G. Nagarajan, *Monatsh. Chem.*, **100**, 1960 (1970), with $\nu_1(a_{1g}) = 187$ cm^{-1}.
(26) C. H. Perry, D. P. Athens, E. F. Young, J. R. Durig, and B. R. Mitchell, *Spectrochim. Acta, Part A*, **23**, 1137 (1967).
(27) J. L. Nims, H. H. Patterson, S. M. Khan, and C. M. Valencia, *Inorg. Chem.*, **12**, 1602 (1973).